ЖЭТФ, 2015, том 148, вып. 5 (11), стр. 908–913 © 2015

# SUB-POISSONIAN PHONON STATISTICS IN AN ACOUSTICAL RESONATOR COUPLED TO A PUMPED TWO-LEVEL EMITTER

*V. Ceban*[*], *M. A. Macovei*[**]

*Institute of Applied Physics, Academy of Sciences of Moldova*
*MD-2028, Chişinău, Moldova*

Received May 25, 2015

The concept of an acoustical analog of the optical laser has been developed recently in both theoretical and experimental works. We here discuss a model of a coherent phonon generator with a direct signature of the quantum properties of sound vibrations. The considered setup is made of a laser-driven quantum dot embedded in an acoustical nanocavity. The system dynamics is solved for a single phonon mode in the steady-state and in the strong quantum dot – phonon coupling regime beyond the secular approximation. We demonstrate that the phonon statistics exhibits quantum features, i. e., is sub-Poissonian.

**DOI**: 10.7868/S0044451015110073

## 1. INTRODUCTION

Sub-Poissonian statistics of vibrational states is a pure quantum propriety of an oscillating system. The domain of this statistics starts at the limit of a classical coherent state having a Poisson-distributed quanta and may end with a pure Fock state at the other limit. Studies on the quanta statistics have already revealed many pure quantum features for different physical systems and remarkable results were achieved in a large spectrum of photonic quantum electrodynamics (QED) applications [1, 2] and in the physics of the Bose–Einstein condensate (BEC) [3, 4]. More recently, successful experiments on cooling and detection of mechanical systems in the near-ground-state domain [5–7] enhanced interest in the research of similar features in the acoustic domain, due to bosonic quantification of sound vibrations.

Earlier experiments on laser generation of coherent phonons in different bulk materials [8–10] were succeeded by new optomechanical and electromechanical setups in phonon QED, achieving important experimental results in an acoustical analog of the optical laser by using piezoelectrically excited electromechanical resonators [11] and laser-driven compound microcavities [12] or trapped ions [13]. In the meantime, theoretical models propose improvements in the background theory of the experiments like the PT-symmetry approach [14] and two-cavity optomechanics [15], as well as new possible setups using vibrating membranes [15, 16], quantum dots embedded in semiconductor lattices [17–19], and BEC under the action of a magnetic cantilever [20]. Moreover, quantum features like sub-Poissonian distributed phonon fields have been already predicted in optomechanical setups based on vibrating mirrors [21, 22] and in single-electron transistors [23] as well as phonon antibunching [19], squeezing [21, 24], and a negative Wigner function of phonon states [25]. In addition to increasing performance of optomechanical devices [26], reports on the state-of-the-art acoustical cavities [27–29] show good phonon trapping in bulk materials with high cavity quality factors, thus leading to the concept of an acoustical analog of photon cavity QED (cQED).

In this article, we study the model of a coherent phonon generator in a setup consisting of a qubit embedded in an acoustical cavity involving strong quantum dot (QD)–phonon-cavity coupling regime. The qubit, i. e., a two-level QD, is driven by an intense laser field and acts as a phonon source. Under the action of laser light, the electron jumps from the QD valence band to the conductance band, leaving a hole in the valence band. The created exciton (electron-hole) represents the QD's excited state and interacts with the acoustic vibrations, thus creating or annihilating phonons in the cavity. We demonstrate that in analo-

[*] E-mail: victor.ceban@phys.asm.md
[**] E-mail: macovei@phys.asm.md

gy with recent experiments in photon cQED [30], the strong qubit–resonator coupling may reveal additional quantum phenomena in the phonon cQED domain. In particular, we show that the steady-state phonon field generated in this regime obeys a sub-Poissonian phonon statistics.

This paper is organized as follows. In Sec. 2, a detailed description of the model is given; after fixing our conventions, we focus on simplifying the system Hamiltonian in order to arrive at an easily solvable master equation for the reduced density operator of the QD–phonon system. In Sec. 3, we present a general overview of the model results and we further discuss the important aspects of the study. A summary is given in Sec. 4.

## 2. THEORETICAL FRAMEWORK

A two-level laser-pumped semiconductor QD is embedded in an acoustical nanocavity (see also Refs. [17, 18]). The QD transition frequency between its ground state $|g\rangle$ and the excited state $|e\rangle$ is denoted by $\omega_{qd}$. The excited QD may spontaneously emit a photon, with the corresponding decay rate $\gamma$ (Fig. 1). In a more realistic case, we introduce the dephasing loss rate through $\gamma_c$. The single-mode cavity phonons of the frequency $\omega_{ph}$ are described by the anihilation ($b$) and creation ($b^\dagger$) operators. The system Hamiltonian is

$$H = \hbar\omega_{qd} S_z + \hbar\omega_{ph} b^\dagger b + \\ + \hbar\Omega\left[(S^+ \exp(-i\omega_L t) + \text{H.c.}\right] + \hbar g S^+ S^- (b^\dagger + b), \quad (1)$$

where the QD operators defined as $S^+ = |e\rangle\langle g|$, $S^- = |g\rangle\langle e|$, and $S_z = (|e\rangle\langle e| - |g\rangle\langle g|)/2$ obey the standard commutation relations for the SU(2) algebra. The first two terms respectively correspond to the unperturbed QD and to the free single-mode phonon Hamiltonians. The third term corresponds to the QD–laser interaction within the rotating wave and dipole approximations, whereas $\omega_L$ is the laser frequency. The last term describes the QD–phonon-cavity interaction with $g$ being the coupling constant.

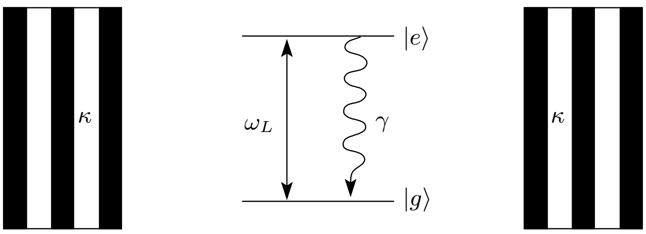


**Fig. 1.** The schematic of the investigated model: a two-level QD is fixed in a multilayered structure forming the acoustical nanocavity. The QD is pumped near resonance with a coherent laser source of the frequency $\omega_L$. The emitter may spontaneously emit a photon at a decay rate $\gamma$; the cavity phonon damping rate is denoted by $\kappa$ (see also Ref. [29])

In what follows, we describe the Hamiltonian in a frame rotating with the laser frequency $\omega_L$ and apply the dressed-state transformation:

$$\begin{aligned} |+\rangle &= \sin\theta|g\rangle + \cos\theta|e\rangle, \\ |-\rangle &= \cos\theta|g\rangle - \sin\theta|e\rangle, \end{aligned} \quad (2)$$

where $2\theta = \arctan(2\Omega/\Delta)$ and $\Delta = \omega_{qd} - \omega_L$ is the detuning of the laser from the QD transition frequency. The dressed-state system Hamiltonian then becomes

$$H = \hbar\bar{\Omega}R_z + \hbar\omega_{ph} b^\dagger b + \hbar g(b^\dagger + b) \times \\ \times \left\{\sin^2\theta R_{--} + \cos^2\theta R_{++} - \frac{\sin(2\theta)}{2}(R^+ + R^-)\right\}, \quad (3)$$

where $\bar{\Omega} = \sqrt{\Omega^2 + (\Delta/2)^2}$. The new QD operators

$$R^+ = |+\rangle\langle -|, \quad R^- = |-\rangle\langle +|,$$

$$R_{++} = |+\rangle\langle +|, \quad R_{--} = |-\rangle\langle -|, \quad R_z = R_{++} - R_{--}$$

satisfy the commutation relations $[R^\pm, R^\mp] = \pm R_z$ and $[R^\mp, R_z] = \pm 2R^\mp$. Again, we perform a unitary transformation of the system Hamiltonian,

$$U(t) = \exp\left[i(\bar{\Omega}R_z + \omega_{ph} b^\dagger b)t\right],$$

and represent it as follows:

$$\begin{aligned} H &= H_{slow} + H_{fast}, \\ H_{slow} &= -\hbar g\frac{\sin(2\theta)}{2} \times \\ &\times \{b^\dagger R^- \exp\left[i(\omega_{ph} - 2\bar{\Omega})t\right] + \text{H.c.}\}, \\ H_{fast} &= \hbar g(\sin^2\theta R_{--} + \cos^2\theta R_{++}) \times \\ &\times \{b^\dagger \exp\left[i\omega_{ph}t\right] + \text{H.c.}\} - \hbar g\frac{\sin(2\theta)}{2} \times \\ &\times \{b^\dagger R^+ \exp\left[i(\omega_{ph} + 2\bar{\Omega})t\right] + \text{H.c.}\}. \end{aligned} \quad (4)$$

Instead of adopting the standard secular approximation [31, 32], we keep the fast rotating terms in the QD–phonon-cavity interaction Hamiltonian. Their main contribution is evaluated as [33, 34]

$$H^{eff}_{fast} = -\frac{i}{\hbar}H_{fast}(t)\int dt'\, H_{fast}(t') = \\ = H_0 - \hbar\bar{\Delta}R_z + \hbar\beta b^\dagger b R_z \quad (5)$$

with

$$\bar{\Delta} = \frac{g^2}{2}\left(\frac{\cos(2\theta)}{\omega_{ph}} - \frac{\sin^2(2\theta)}{4(\omega_{ph}+2\bar{\Omega})}\right)$$

and

$$\beta = g^2\frac{\sin^2(2\theta)}{4(\omega_{ph}+2\bar{\Omega})}.$$

Here, $H_0$ is a constant that can be dropped because it does not contribute to the system dynamics. We note that the coupling regimes are related not only to the QD–phonon-cavity coupling constant $g$ but also to the contribution coming from fast rotating terms, i. e., $\bar{\Delta}$ and $\beta$, proportional to $g^2$. Consequently, for low QD–phonon coupling strengths $g$, the contribution of fast rotating terms can be neglected, i. e., $\{\bar{\Delta},\beta\} = 0$. For strong QD-phonon coupling regimes, the secular approximation is no longer justified and the contribution of $H_{fast}^{eff}$ plays a role that we consider below. Thus, the final Hamiltonian $H = H_{slow} + H_{fast}^{eff}$ is

$$H = \hbar(\omega_{ph} - 2\bar{\Omega})b^\dagger b - \hbar\bar{\Delta}R_z + \hbar\beta b^\dagger bR_z - \hbar g\frac{\sin(2\theta)}{2}\left(b^\dagger R^- + R^+ b\right). \quad (6)$$

To solve the QD–phonon system dynamics, we use the density matrix formalism for the reduced density operator $\rho$:

$$\dot{\rho} = -\frac{i}{\hbar}[H,\rho] + \mathcal{L}_{qd}\rho + \mathcal{L}_{ph}\rho, \quad (7)$$

where the Liouville superoperators $\mathcal{L}_{qd}$ and $\mathcal{L}_{ph}$ respectively describe the QD and phonon dissipative effects. In the bare-state representation, the QD dissipation processes are expressed by the spontaneous emission term [31, 32, 35]

$$\mathcal{L}_{qd}\rho = -\gamma[S^+, S^-\rho] - \gamma_c[S_z, S_z\rho] + \text{H.c.}$$

In the dressed-state basis and within the secular approximation (i. e., for $2\bar{\Omega} \gg \gamma$), the same processes are described by three terms [36] determined by the QD dressed-state decay rates:

$$\gamma_+ = \gamma\cos^4\theta + \frac{1}{4}\gamma_c\sin^2(2\theta),$$

$$\gamma_- = \gamma\sin^4\theta + \frac{1}{4}\gamma_c\sin^2(2\theta),$$

$$\gamma_0 = \frac{1}{4}[\gamma\sin^2(2\theta) + \gamma_c\cos^2(2\theta)].$$

Therefore,

$$\mathcal{L}_{qd}\rho = -\gamma_+[R^+, R^-\rho] - \gamma_-[R^-, R^+\rho] - \gamma_0[R_z, R_z\rho] + \text{H.c.} \quad (8)$$

The phonons from the multilayered acoustical cavity are allowed to interact with the environmental thermal reservoir. In the rotating wave approximation, this process is described by two terms respectively corresponding to the cavity damping and pumping effects at a rate proportional to $\kappa = \omega_{ph}/Q$ determined by the cavity quality factor $Q$ [31]:

$$\mathcal{L}_{ph}\rho = -\kappa(1+\bar{n})[b^\dagger, b\rho] - \kappa\bar{n}[b, b^\dagger\rho] + \text{H.c.} \quad (9)$$

Here, $\bar{n}$ is the mean thermal phonon number corresponding to the frequency $\omega_{ph}$ and the environmental temperature $T$.

Once the master equation is determined by Eqs. (6)–(9), it is solved by projecting the density operator first in the QD basis and then in the phonon field basis [37]. The projection in the QD dressed-state basis leads after some rearrangements to a system of six coupled differential equations involving the variables

$$\begin{aligned}
&\rho^{(1)} = \rho_{++} + \rho_{--}, \quad \rho^{(2)} = \rho_{++} - \rho_{--},\\
&\rho^{(3)} = b^\dagger\rho_{+-} - \rho_{-+}b, \quad \rho^{(4)} = b^\dagger\rho_{+-} + \rho_{-+}b,\\
&\rho^{(5)} = \rho_{+-}b^\dagger - b\rho_{-+}, \quad \rho^{(6)} = \rho_{+-}b^\dagger + b\rho_{-+},
\end{aligned} \quad (10)$$

where $\rho_{i,j} = \langle i|\rho|j\rangle$, $\{i,j \in |+\rangle, |-\rangle\}$ are the QD density matrix elements. Finally, the projection in the phonon Fock state basis $\{|n\rangle\}$ gives a set of infinite differential equations, namely,

$$\begin{aligned}
\dot{P}_n^{(1)} = {}& ig\frac{\sin(2\theta)}{2}\left(P_n^{(3)} - P_n^{(5)}\right) - 2\kappa(1+\bar{n}) \times\\
&\times\left(nP_n^{(1)} - (n+1)P_{n+1}^{(1)}\right) -\\
&- 2\kappa\bar{n}\left((n+1)P_n^{(1)} - nP_{n-1}^{(1)}\right),
\end{aligned} \quad (11)$$

$$\begin{aligned}
\dot{P}_n^{(2)} = {}& -ig\frac{\sin(2\theta)}{2}\left(P_n^{(3)} + P_n^{(5)}\right) -\\
&- 2(\gamma_+ - \gamma_-)P_n^{(1)} - 2(\gamma_+ + \gamma_-)P_n^{(2)} -\\
&- 2\kappa(1+\bar{n})\left(nP_n^{(2)} - (n+1)P_{n+1}^{(2)}\right) -\\
&- 2\kappa\bar{n}\left((n+1)P_n^{(2)} - nP_{n-1}^{(2)}\right),
\end{aligned} \quad (12)$$

$$\begin{aligned}
\dot{P}_n^{(3)} = {}& ign\frac{\sin(2\theta)}{2}\left(P_n^{(1)} - P_n^{(2)} - P_{n-1}^{(1)} - P_{n-1}^{(2)}\right) -\\
&- i\left(\beta(2n-1) - \delta\right)P_n^{(4)} -\\
&- (\gamma_+ + \gamma_- + 4\gamma_0)P_n^{(3)} -\\
&- \kappa(1+\bar{n})\left((2n-1)P_n^{(3)} - 2(n+1)P_{n+1}^{(3)} + 2P_n^{(5)}\right) -\\
&- \kappa\bar{n}\left((2n+1)P_n^{(3)} - 2nP_{n-1}^{(3)}\right),
\end{aligned} \quad (13)$$

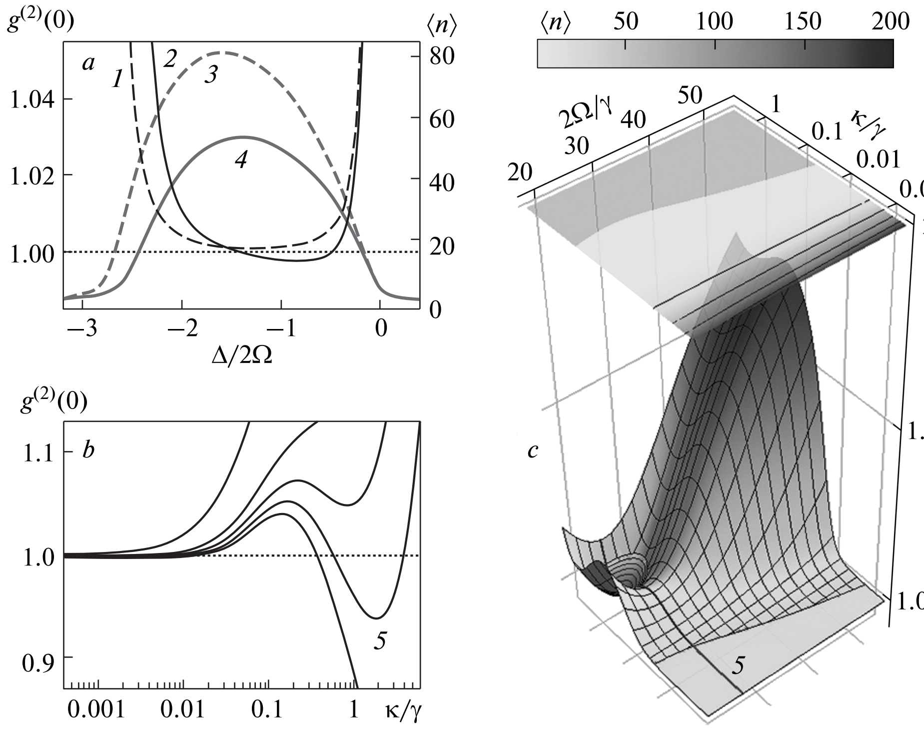


**Fig. 2.** ($a$) The second-order phonon–phonon correlation function $g^{(2)}(0)$ (curves *1* and *2*) and the mean phonon number in the cavity $\langle n\rangle$ (curves *3* and *4*) as functions of the QD–laser detuning $\Delta$ normalized by the Rabi frequency $2\Omega$ beyond the secular approximation (solid lines) and within the secular approximation (dashed lines). Here, $\bar{n} = 0.04$, $2\Omega/\gamma = 25$, and $\kappa/\gamma = 5\cdot 10^{-3}$. ($b$) $g^{(2)}(0)$ as a function of the normalized damping rate $\kappa/\gamma$ for thermal baths at different temperatures and for $2\Omega/\gamma = 25$ and $\Delta/2\Omega = -0.7$. Here, from top to bottom, $\bar{n} = 0.64, 0.16, 0.08, 0.04, 0.01$. ($c$) $g^{(2)}(0)$ (3D surface) and $\langle n\rangle$ (density plot) as functions of $\kappa/\gamma$ and $2\Omega/\gamma$. Here, $\bar{n} = 0.04$ and $\Delta/2\Omega = -0.7$. The plot regions corresponding to $g^{(2)}(0) > 1$ and $g^{(2)}(0) < 1$ are represented in different mesh styles. Other parameters are: $\gamma_c/\gamma = 0.1$, $g/\gamma = 15$, and $\omega_{ph}/\gamma = 35$

$$\begin{aligned}\dot{P}_n^{(4)} &= -i\left(\beta(2n-1)-\delta\right)P_n^{(3)} - \\ &- (\gamma_+ + \gamma_- + 4\gamma_0)P_n^{(4)} - \\ &-\kappa(1+\bar{n})\left((2n-1)P_n^{(4)} - 2(n+1)P_{n+1}^{(4)} + 2P_n^{(6)}\right) - \\ &- \kappa\bar{n}\left((2n+1)P_n^{(4)} - 2nP_{n-1}^{(4)}\right), \end{aligned} \quad (14)$$

$$\begin{aligned}\dot{P}_n^{(5)} &= -ig(n+1)\frac{\sin(2\theta)}{2}\times \\ &\times\left(P_n^{(1)} + P_n^{(2)} - P_{n+1}^{(1)} + P_{n+1}^{(2)}\right) - \\ &- i\left(\beta(2n+1)-\delta\right)P_n^{(6)} - \\ &- (\gamma_+ + \gamma_- + 4\gamma_0)P_n^{(5)} - \kappa(1+\bar{n})\times \\ &\times\left((2n+1)P_n^{(5)} - 2(n+1)P_{n+1}^{(5)}\right) - \\ &- \kappa\bar{n}\left((2n+3)P_n^{(5)} - 2nP_{n-1}^{(5)} - 2P_n^{(3)}\right), \end{aligned} \quad (15)$$

$$\begin{aligned}\dot{P}_n^{(6)} &= -i\left(\beta(2n+1)-\delta\right)P_n^{(5)} - (\gamma_+ + \gamma_- + 4\gamma_0)P_n^{(6)} - \\ &- \kappa(1+\bar{n})\left((2n+1)P_n^{(6)} - 2(n+1)P_{n+1}^{(6)}\right) - \\ &- \kappa\bar{n}\left((2n+3)P_n^{(6)} - 2nP_{n-1}^{(6)} - 2P_n^{(4)}\right). \end{aligned} \quad (16)$$

Here, $P_n^{(i)} = \langle n|\rho^{(i)}|n\rangle$ and $\delta = \omega_{ph} - 2\bar{\Omega} + 2\bar{\Delta}$.

In the next section, we describe the cavity phonon dynamics in a steady state via a second-order phonon–phonon correlation function and the mean phonon number.

## 3. RESULTS AND DISCUSSION

The mean phonon number in the cavity mode is expressed as

$$\langle n\rangle = \langle b^\dagger b\rangle = \sum_{n=0}^{\infty} nP_n^{(1)}. \quad (17)$$

The nanocavity second-order phonon–phonon correlation function is defined as usual [38],

$$g^{(2)}(0) = \frac{\langle b^\dagger b^\dagger b b\rangle}{\langle b^\dagger b\rangle^2} = \frac{1}{\langle n\rangle^2}\sum_{n=0}^{\infty} n(n-1)P_n^{(1)}. \qquad (18)$$

System of equations (11)–(16) and the infinite series in expressions (17)–(18) must be truncated at a particular value $n = N_{max}$ such that the variables of interest remain unchanged if $N_{max}$ is further increased [39].

In what follows, we study the system in the steady-state regime, $\dot{P}_n^{(i)} = 0$ for $i = 1, \ldots, 6$. The second-order correlation function given by Eq. (18) and the mean phonon number in Eq. (17) are used to describe the phonon field behavior in the acoustical cavity mode [38]. Once truncated, the system of coupled equations (11)–(16) is solved by setting the model parameters $\{\gamma, \gamma_c, g, \omega_{ph}, \kappa, \bar{n}, \Omega\}$ and $\Delta$.

A general overview of the steady-state system behavior in the strong-coupling regime or within the secular approximation, i.e., when $\{\bar{\Delta}, \bar{\beta} = 0\}$, is presented in Fig. 2. The phonon field statistics is described by a second-order correlation function $g^{(2)}(0)$ such that $g^{(2)}(0) = 1$ describes the Poissonian phonon distribution and $g^{(2)}(0) < 1$ a sub-Poissonian phonon statistics. We observe that moderate laser–QD coupling strengths $\Omega$ as well as lower temperatures give rise to a more prominent sub-Poissonian phonon statistics. Furthermore, beyond the secular approximation, the phonon statistics exhibits quantum features, i.e., $g^{(2)}(0) < 1$ (cf. the corresponding curves in Fig. 2*a*) and the effect is more pronounced for stronger QD–phonon coupling strengths. Figure 2*b* shows the second-order phonon–phonon correlation function beyond the secular approximation as a function of $\kappa/\gamma$. Here, again, we have a quantum phonon effect, i.e., a sub-Poissonian phonon statistics around $\kappa > \gamma$. Thus, the contribution to the system dynamics of the fast rotating terms $H^{eff}_{fast}$ evaluated by Eq. (5) are essential for a sub-Poissonian quantum feature (see Fig. 2). In Fig. 3, we compare our result within and beyond the secular approximation. The second-order correlation function estimated in both cases converges for higher and smaller cavity damping rates. However, for lower values of $\kappa/\gamma$, quantum features are proper only beyond the secular approximation (see the inset in Fig. 3). Furthermore, the mean phonon number decreases in this particular case although it is quite high comparing to the $\kappa > \gamma$ situation.

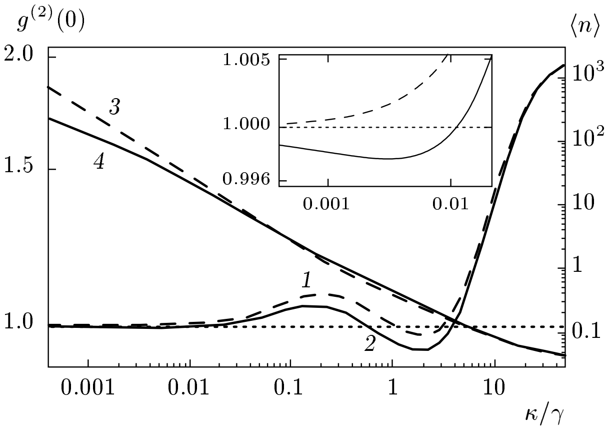


**Fig. 3.** The second-order phonon–phonon correlation function $g^{(2)}(0)$ (curves *1* and *2*) and the mean phonon number in the cavity mode $\langle n\rangle$ (curves *3* and *4*) as functions of the cavity damping rate $\kappa$ normalized by the spontaneous emission rate $\gamma$. The solid curves are beyond the secular approximation whereas the dashed ones are within the secular approximation. Here, $2\Omega/\gamma = 25$, $\Delta/(2\Omega) = -0.7$, $\bar{n} = 0.04$, $\gamma_c/\gamma = 0.1$, $g/\gamma = 15$, and $\omega_{ph}/\gamma = 35$. The solid curve *2* is identical to the curves *5* in Fig. 2*b,c*. The inset represents a closer look at the behavior of the second-order correlation functions in the regions around $10^{-3} \le \kappa/\gamma \le 10^{-2}$

## 4. SUMMARY

In summary, we have investigated the phonon quantum statistics in an acoustical nanocavity. A laser-pumped two-level quantum dot is embedded in the cavity contributing to the phonon quantum dynamics. We have demonstrated that stronger QD–phonon-cavity coupling regimes lead to quantum features of the cavity phonon field in the steady state. This QD–cavity interaction regime requires going beyond the secular approximation. Ignoring this fact would lead to an erroneous estimation of the phonon statistics for some parameter domains.

We are grateful to financial support via the research Grant No. 13.820.05.07/GF.

## REFERENCES


1. G. Rempe, F. Schmidt-Kaler, and H. Walther, Phys. Rev. Lett. **64**, 2783 (1990).

2. A. V. Poshakinskiy and A. N. Poddubny, Zh. Eksp. Teor. Fiz. **145**, 237 (2014).

3. C.-S. Chuu, F. Schreck, T. P. Meyrath et al., Phys. Rev. Lett. **95**, 260403 (2005).

4. Th. Jacqmin, J. Armijo, T. Berrada et al., Phys. Rev. Lett. **106**, 230405 (2011).

5. T. Rocheleau, T. Ndukum, C. Macklin et al., Nature (London) **463**, 72 (2010).

6. A. D. O'Connell, M. Hofheinz, M. Ansmann et al., Nature (London) **464**, 697 (2010).

7. J. Chan, T. P. Mayer Alegre, A. H. Safavi-Naeini et al., Nature (London) **478**, 89 (2011).

8. W. Kütt, W. Albrecht, and H. Kurz, IEEE J. Quant. Electron. **28**, 2434 (1992).

9. A. Bartels, Th. Dekorsy, and H. Kurz, Phys. Rev. Lett. **82**, 1044 (1999).

10. Y. Ezzahri, S. Grauby, J. M. Rampnoux et al., Phys. Rev. B **75**, 195309 (2007).

11. I. Mahboob, K. Nishiguchi, A. Fujiwara, and H. Yamaguchi, Phys. Rev. Lett. **110**, 127202 (2013).

12. I. S. Grudinin, H. Lee, O. Painter, and K. J. Vahala, Phys. Rev. Lett. **104**, 083901 (2010).

13. K. Vahala, M. Hermann, S. Knünz et al., Nature Phys. **5**, 682 (2009).

14. H. Jing, S. K. Özdemir, Xin-You Lü et al., Phys. Rev. Lett. **113**, 053604 (2014).

15. H. Wang, Z. Wang, J. Zhang et al., Phys. Rev. A **90**, 053814 (2014).

16. H. Wu, G. Heinrich, and F. Marquardt, New J. Phys. **15**, 123022 (2013).

17. J. Kabuss, A. Carmele, T. Brandes, and A. Knorr, Phys. Rev. Lett. **109**, 054301 (2012).

18. J. Kabuss, A. Carmele, and A. Knorr, Phys. Rev. B **88**, 064305 (2013).

19. R. Okuyama, M. Eto, and T. Brandes, New J. Phys. **15**, 083032 (2013).

20. A. B. Bhattacherjee and T. Brandes, Canad. J. Phys. **91**, 639 (2013).

21. T. Figueiredo Roque and A. Vidiella-Barranco, arXiv: 1406.1987v3 [quant-ph].

22. P. D. Nation, Phys. Rev. A **88**, 053828 (2013).

23. M. Merlo, F. Haupt, F. Cavaliere, and M. Sassetti, New J. Phys. **10**, 023008 (2008).

24. A. Kronwald, F. Marquardt, and A. A. Clerk, Phys. Rev. A **88**, 063833 (2013).

25. J. Qian, A. A. Clerk, K. Hammerer, and F. Marquardt, Phys. Rev. Lett. **109**, 253601 (2012).

26. M. Aspelmeyer, T. J. Kippenberg, and F. Marquardt, Rev. Mod. Phys. **86**, 1391 (2014).

27. M. Trigo, A. Bruchhausen, A. Fainstein et al., Phys. Rev. Lett. **89**, 227402 (2002).

28. N. D. Lanzillotti-Kimura, A. Fainstein, B. Perrin et al., Phys. Rev. B **83**, 201103 (2011).

29. Ö. O. Soykal, R. Ruskov, and Ch. Tahan, Phys. Rev. Lett. **107**, 235502 (2011).

30. H. Kim, Th. C. Shen, K. Roy-Choudhury et al., Phys. Rev. Lett. **113**, 027403 (2014).

31. M. Scully and M. S. Zubairy, *Quantum Optics*, Cambridge Univ. Press, Cambridge (1997).

32. M. Kiffner, M. Macovei, J. Evers, and C. H. Keitel, Progr. Opt. **55**, 85 (2010).

33. D. F. V. James, Fortschr. Phys. **48**, 823 (2000).

34. R. Tan, G.-X. Li, and Z. Ficek, Phys. Rev. A **78**, 023833 (2008).

35. S. Y. Kilin, JETP **51**, 1081 (1980).

36. M. Macovei, J. Evers, G.-X. Li, and C. H. Keitel, Phys. Rev. Lett. **98**, 043602 (2007).

37. T. Quang, P. L. Knight, and V. Buzek, Phys. Rev. A **44**, 6092 (1991).

38. R. J. Glauber, Phys. Rev. **130**, 2529 (1963).

39. C. Ginzel, H.-J. Briegel, U. Martini et al., Phys. Rev. A **48**, 732 (1993).